

NACA RM L56D11a

0697


NACATECH LIBRARY KAFB, NM
0144214

RESEARCH MEMORANDUM

TRANSONIC INVESTIGATION AT LIFTING CONDITIONS
OF STREAMLINE CONTOURING IN THE SWEEPBACK-WING—FUSELAGE
JUNCTURE IN COMBINATION WITH THE
TRANSONIC AREA RULE

By William E. Palmer, Robert R. Howell,
and Albert L. Braslow

Langley Aeronautical Laboratory
Langley Field, Va.

CLASSIFIED DOCUMENT

This material contains information affecting the National Defense of the United States within the meaning of the espionage laws, Title 18, U.S.C., Secs. 793 and 794, the transmission or revelation of which in any manner to an unauthorized person is prohibited by law.

NATIONAL ADVISORY COMMITTEE
FOR AERONAUTICS

WASHINGTON

July 20, 1956



0144214

NACA RM L56D11a

NATIONAL ADVISORY COMMITTEE FOR AERONAUTICS

RESEARCH MEMORANDUM

TRANSONIC INVESTIGATION AT LIFTING CONDITIONS
OF STREAMLINE CONTOURING IN THE SWEPTBACK-WING—FUSELAGE
JUNCTURE IN COMBINATION WITH THE

TRANSONIC AREA RULE

By William E. Palmer, Robert R. Howell,
and Albert L. Braslow

SUMMARY

An investigation has been made in the Langley transonic blowdown tunnel at Mach numbers between 0.8 and 1.3 to determine the possible drag reductions at angles of attack to 12° due to contouring the fuselage of a 45° sweptback-wing—fuselage combination such that the wing-fuselage juncture conformed approximately to the surface streamline shape that would exist over a wing of infinite span at a given lift coefficient. The longitudinal distribution of cross-sectional area of the four configurations tested conformed to the transonic area rule. One configuration had an axisymmetric fuselage and the other three fuselages were streamlined for lift coefficients of 0, 0.1, and 0.4. Lift, drag, and pitching-moment characteristics were determined at a Reynolds number of approximately 3×10^6 based on the wing mean aerodynamic chord.

The results of the investigation indicate that all streamline contoured configurations had generally lower drag than the axisymmetric model throughout the range of test conditions. The configuration streamlined for 0.1 lift coefficient showed the greatest improvement at low lift and had reductions in drag coefficient up to approximately 0.007 as compared with the configuration having the axisymmetric fuselage. Drag reductions were generally greater at lifting conditions than at zero lift. The configuration designed for 0.4 lift coefficient did not improve the drag characteristics appreciably except in a very limited range of Mach number and lift coefficient near design. This configuration did have a higher lift-curve slope and a more rearward aerodynamic center at supersonic speeds, however, and had a shift in pitching moment which was in a direction to reduce drag due to trim.

INTRODUCTION

The concept of shaping the fuselage of a sweptback-wing—fuselage combination in such a way as to combine the curvature of the streamlines over an infinite sweptback wing with the longitudinal area distribution obtained from application of either the transonic area rule or the supersonic area rule was advanced in references 1 and 2, respectively. Experimental data are presented in these reports which show that this method of fuselage shaping resulted in reductions in zero-lift pressure drag coefficient significantly greater than those obtained through the use of axisymmetric application of either the transonic or supersonic area rules alone.

The purpose of the present investigation was twofold: (1) to determine whether the drag improvements of the wing-fuselage configuration having a fuselage contoured with the combination of the zero-lift streamline and area rule could be maintained at lifting conditions and (2) to determine whether the drag characteristics of the wing-fuselage configuration could be improved further at lifting conditions by utilizing a streamline contour corresponding to a given lift coefficient. Accordingly, tests were made in the Langley transonic blowdown tunnel through a range of lift coefficients of sweptback-wing—fuselage configurations having fuselages contoured in accordance with a combination of transonic area rule and streamline shape designed for lift coefficients of 0, 0.1, and 0.4. For purposes of comparison, the axisymmetrical-area-rule indented configuration of reference 1 was tested through the same range of lift coefficient.

The general wing-body configuration consisted of a sweptback wing having a quarter-chord sweep of 45° , aspect ratio 4, taper ratio 0.6, and NACA 65A006 airfoil sections in the stream direction. The Mach number was varied from 0.8 to 1.3 at a Reynolds number of approximately 3.0×10^6 based on the wing mean aerodynamic chord.

SYMBOLS

C_D	drag coefficient,	$\frac{\text{Drag}}{q_\infty S}$
C_L	lift coefficient,	$\frac{\text{Lift}}{q_\infty S}$
C_{L_α}	lift-curve slope,	$\frac{dC_L}{d\alpha}$

C_m	pitching-moment coefficient, $\frac{\text{Pitching moment about } \bar{c}/4}{q_o S \bar{c}}$
C_p	pressure coefficient, $\frac{p - p_o}{q_o}$
\bar{c}	wing mean aerodynamic chord
c	wing chord
M	free-stream Mach number
h	body height from center line, in.
p	static pressure at a point on airfoil surface
p_o	free-stream static pressure
q_o	free-stream dynamic pressure, $\frac{1}{2} \rho_o V_o^2$
r	body radius
S	total wing area, 12.96 sq in.
V_o	free-stream velocity
V_N	component of V_o normal to 0.5-chord line
V_T	component of V_o parallel to 0.5-chord line
w	body width from center line in plane of wing, in.
x	distance measured from fuselage-nose leading edge parallel to body center line, in.
x', y'	distances measured normal to and parallel to sweep line of infinite-span wing with origin at wing leading edge (fig. 3), in.
α	angle of attack, deg
Λ	angle of sweep of the wing of infinite span, deg
ρ_o	free-stream density
γ	ratio of specific heat at constant pressure to specific heat at constant volume

MODELS, APPARATUS, AND TESTS

Models

Four bodies of fineness ratio 6.7 were tested in combination with a wing of aspect ratio 4, taper ratio 0.6, 45° sweepback of the quarter-chord line, and NACA 65A006 airfoil sections parallel to the model center line. The wing was mounted on the fuselage in the midwing position with zero angle of incidence and zero dihedral. The ratio of body frontal area to wing area was 0.136. The forebody of each of the fuselages was defined by the relation $r \propto x^{1/2}$ and was of fineness ratio 3.0. The longitudinal distribution of cross-sectional area was the same for all four configurations and is given in reference 1.

Axisymmetric design.- This configuration had a body which was indented axisymmetrically to offset the volume of the wing according to the transonic-area-rule principle (ref. 3). Body radii are given in reference 1 along with zero-lift drag data of the model tested without transition fixed by roughness strips.

Zero-lift design.- Derivation of the zero-lift design fuselage is described in detail in reference 1 where zero-lift drag data are presented. Also presented in reference 1 are the detailed dimensions and ordinates for this configuration. It should be noted that the cross-sectional shape of this fuselage was derived from an arbitrary redistribution of body volume as required to maintain the longitudinal area distribution.

Lifting designs ($C_L = 0.1$ and $C_L = 0.4$).- Sketches of the fuselages designed for lift coefficients of 0.1 and 0.4 are presented in figure 1 and photographs of the models are presented as figure 2. Unpublished experimental surface pressures measured on an NACA 65A009 airfoil section at a Mach number of about 0.7 (design Mach number ≈ 1.0) and obtained in the Langley 4- by 19-inch semiopen tunnel were used in conjunction with the sweep of the 0.5-chord line in the calculation of the streamline shape over the wing of infinite span. The effects of wing taper and the presence of the wing tips and body on the pressures were not considered.

The following procedure was used to obtain the streamline shape. The local resultant velocity at any point on the infinite-span wing was taken to be the sum of the local velocity normal to the sweep line and the tangential component of the free-stream velocity. The local velocity normal to the sweep line V_N' was obtained from the two-dimensional pressure-distribution data by use of the relation

~~CONFIDENTIAL~~

$$\frac{V_{N'}}{V_N} = \sqrt{1 - \frac{2}{(\gamma - 1)M_N^2} \left[\left(C_p \frac{\gamma}{2} M_N^2 + 1 \right)^{\frac{\gamma-1}{\gamma}} - 1 \right]}$$

where M_N and V_N are the Mach number and velocity components of the free-stream flow normal to the sweep line and C_p is the two-dimensional pressure coefficient. The tangential-velocity component $V_T' = V_T = V_O \sin \Lambda$ was assumed to be constant throughout the flow field; thus, the lateral slope of the velocity vector at any point is given by

$$\frac{dy'}{dx'} = \frac{V_T'}{V_{N'}} = \frac{V_O \sin \Lambda}{V_O \cos \Lambda \sqrt{1 - \frac{2}{(\gamma - 1)M_O^2 \cos^2 \Lambda} \left[\left(C_p \frac{\gamma}{2} M_O^2 \cos^2 \Lambda + 1 \right)^{\frac{\gamma-1}{\gamma}} - 1 \right]}}$$

where the subscript o denotes free-stream conditions and the prime denotes local conditions at any point in the field. Hence, the lateral displacement at any point in terms of the chord of the wing of infinite span is

$$\frac{y'}{c} = \int \frac{dy'}{dx'} d\left(\frac{x'}{c}\right) = \tan \Lambda \int_0^1 \frac{d\left(\frac{x'}{c}\right)}{\sqrt{1 - \frac{2}{(\gamma - 1)M_O^2 \cos^2 \Lambda} \left[\left(C_p \frac{\gamma}{2} M_O^2 \cos^2 \Lambda + 1 \right)^{\frac{\gamma-1}{\gamma}} - 1 \right]}}$$

Thus, the surface streamline (and body) contour is given in terms of a system of rectilinear axes normal to and parallel with the wing sweep line as shown in figure 3.

For the lifting cases, the streamlines on the upper and lower surfaces of the wing are not the same. The paths of the two surface streamlines are such that there results a displacement of the streamlines at the wing trailing edge. When the fuselage was shaped to conform to the different shapes on the two surfaces of the wing, a shelf was formed at the trailing edge of the wing in order to fair the streamlines to the general fuselage plan form. For the present case, an arbitrary fairing was used. As contrasted with the arbitrary cross-sectional shape for the zero-lift design, semi-elliptical cross-sectional shapes were used for the lifting designs on both the top and bottom of the fuselages to obtain the streamline contours in the fuselage sides (fig. 1) and the desired longitudinal cross-sectional

area distribution. Ordinates for these fuselage configurations are presented in tables I and II.

Apparatus

The tests were made in the Langley transonic blowdown tunnel which has a slotted test section with an octagonal cross-sectional shape measuring 26 inches between flats. The models were supported by a three-component internal strain-gage balance which was sting-mounted in the tunnel. Force and moment data were recorded by photographing self-balancing potentiometers. Base pressures were measured by inserting an open-end tube through the center of the sting into an open section of the balance. The pressure so measured was the average static pressure in the annular opening around the sting in the plane of the model base. All pressure data were recorded by quick-response flight-type pressure recorders.

Tests

The tests were made through a range of Mach number from 0.8 to 1.3 at Reynolds numbers ranging from 2.5×10^6 to 3.0×10^6 based on the mean aerodynamic chord of the wing. Data were obtained at angles of attack from approximately 0° to 12° , and the measured angles were corrected for sting and balance deflection due to aerodynamic load.

All the tests of the present investigation were made with roughness strips on the fuselage forebody and on both surfaces of the wing near the leading edge in order to eliminate the effects on the aerodynamic characteristics of possible changes in the extent of laminar flow on the model. The roughness strips consisted of 0.001- to 0.002-inch-diameter carborundum particles blown to a uniform density on a strip of thinned shellac. The strip on the fuselage was 1/4 inch wide and was located 10 percent of the body length behind the nose. The strips on the wing were 1/8 inch wide and were located at 10 percent of the local chord behind the wing leading edge.

From previous tests of models of the same size in the Langley transonic blowdown tunnel, it appears that the results may be influenced by tunnel-wall reflections through a range of Mach number between about 1.04 and about 1.18. No data are presented for this Mach number range. For the present model-to-tunnel size ratio, reference 4 indicates that tunnel boundary effects should be negligible at subsonic speeds.

The drag data measured at Mach numbers greater than 1.18 were corrected for buoyancy effects resulting from longitudinal gradients in the test section Mach number.

RESULTS AND DISCUSSION

Lift and Pitching-Moment Comparison

The measured lift and pitching-moment coefficients are presented in figures 4 and 5, respectively. A comparison of the slopes of the lift coefficient against angle of attack and pitching-moment coefficient against lift coefficient are presented in figures 6 and 7, respectively. The increment of the curves used to determine the slopes was between lift coefficients of 0 and 0.2.

The lift-curve slope (fig. 6) did not change appreciably with variation of fuselage design with the exception of the design for a lift coefficient of 0.4. The $C_L = 0.4$ design exhibited significantly higher values of C_{L_α} in the Mach number range between about 0.9 and about 1.25.

By comparing figure 5(d) with figures 5(a), 5(b), and 5(c), it is seen that there is a shift in the pitching-moment coefficient of about 0.02 at zero lift for the design for a lift coefficient of 0.4. This shift in zero-lift moment is in the direction to reduce the drag due to trim of the configuration at moderate lift. There was no appreciable difference in the pitching-moment characteristics of the other configurations. Figure 7 shows that, at subsonic speeds, the values of dC_m/dC_L are about the same for all configurations. At supersonic speeds, however, the $C_L = 0.4$ design had a more rearward aerodynamic center than the other configurations and hence a greater change in static margin in traversing from subsonic to supersonic speeds.

Drag Comparison

The drag polars for the individual configurations are presented in figure 8. The drag data were adjusted to a condition of free-stream static pressure at the model base. By superposition of the test results for the different configurations, it was found that the general scatter of drag data points obtained for each configuration was less than the differences in mean drag between the configurations. The increments in drag coefficients as obtained from the faired curves presented, therefore, are considered to be much more accurate than might be indicated by consideration of the scatter of test points alone. In order to show a comparison of the drag variations with Mach number at constant lift coefficients of 0, 0.2, and 0.4, cross plots of the faired curves of figure 8 are presented in figure 9.

Zero-lift drag.- The general zero-lift level of the subsonic drag coefficients of the four configurations investigated is measurably greater

~~CONFIDENTIAL~~

than the estimated viscous drag of an equivalent flat plate with fully turbulent flow. Results of an unpublished investigation (obtained in the Langley low-turbulence pressure tunnel) of distributed three-dimensional roughness particles of the type used in the present investigation to fix transition indicate that the size of the roughness used was several times greater than that required to fix transition. The increase in subsonic drag coefficient over that of turbulent skin friction, therefore, is most likely primarily caused by the drag of the roughness itself. Inasmuch as the roughness strips used were carefully controlled in geometry and composition, it is believed that the measured differences in drag between the various configurations are reliable. Several repeat tests also indicate that the measured differences were not due to instrument malfunction or blowing off of roughness particles by the airstream during the course of the tests.

Inasmuch as the subsonic drag increments between the different configurations are not due to changes in viscous drag, they must be due to changes in pressure drag. These differences in pressure drag between the various body contours are probably influenced by an interaction with the boundary layer of localized shock waves which schlieren surveys showed to exist around the fuselage at Mach numbers as low as 0.8.

These measured subsonic drag differences for the configurations with artificially fixed transition suggested a reexamination of the results obtained for two of the same configurations in reference 1. These configurations, the axisymmetric indented fuselage design and the zero-lift streamline-contoured fuselage design, were tested in reference 1 with supposedly free transition. The recent investigation of the effects of distributed three-dimensional roughness particles previously referred to indicate that for the combination of model size and Reynolds number per foot used in reference 1, surface roughness of the order of 0.0002 inch would be sufficient to cause premature boundary-layer transition from laminar to turbulent flow. It is extremely unlikely that the models of reference 1 were tested with surfaces having this degree of smoothness so that it appears that little, if any, laminar flow existed. In fact, the general level of subsonic drag coefficient of the models of reference 1 is approximately equal to the estimated viscous drag for fully turbulent flow. A comparison of the difference in drag coefficient between the two configurations, as obtained in the present tests, with the difference obtained in reference 1 is presented in figure 10. The increments at both subsonic and supersonic speeds were the same for both investigations. This is a further indication that the variation in subsonic drag-coefficient level between these two configurations is due to a difference in pressure drag and not to variations in extent of laminar flow as was supposed in reference 1.

The apparent reductions in drag coefficient at zero lift afforded by the design for a lift coefficient of 0.1 as compared with the zero-lift

contoured design is not clearly understood. It appears remote that such drag differences can be afforded by only the small difference in fuselage-wing-juncture contour between these two configurations. The drag reduction may possibly be attributed to secondary effects produced by the previously noted differences in cross-sectional shape between these two configurations.

The zero-lift drag of the design for a lift coefficient of 0.4 was generally higher than that for the other streamline-contoured configurations as might have been expected. These results provide an indication of the possible penalty at zero lift which may result from attempts to contour a fuselage to provide low drag at a specific lift coefficient appreciably greater than zero.

Generally, it may be noted that all the streamline-contoured configurations had significantly lower zero-lift drag than the axisymmetric configuration. At the design Mach number $M = 1.0$, the zero-lift contour afforded a reduction in drag coefficient of about 0.004 relative to the axisymmetric-area-rule indented configuration. This reduction in drag coefficient diminished to about 0.003 at $M = 1.3$. The 0.1-lift-coefficient design generally afforded the lowest zero-lift drag coefficient level of all the configurations. As was mentioned previously, the fact that the 0.1-lift-coefficient design had lower drag than the zero-lift design at zero lift may possibly be associated with the difference in cross-sectional shape. As previously pointed out, the 0.4-lift-coefficient design had the highest zero-lift drag of all the streamlined configurations tested.

It should be noted that the magnitude of drag reduction is influenced by the ratio of fuselage frontal area to wing plan-form area. The success of the streamline contouring depends on how well the fuselage aerodynamically separates the two swept-wing panels. Hence, a decrease in relative fuselage size would be expected to decrease the effectiveness of the streamline contouring concept.

Drag at lifting conditions.- It may be noted from figure 9 that, relative to the axisymmetrical-area-rule configuration, any reduction in drag attained at zero lift due to streamline contouring was maintained or increased in the moderate lift-coefficient range. The configuration designed for $C_L = 0.1$ showed generally the greatest improvement at low lift and produced reductions in drag coefficient up to about 0.007 as compared with the axisymmetric configuration.

Except for a narrow range of Mach number and lift coefficient near design, the 0.4-lift-coefficient design generally had the highest drag of the three streamline-contoured configurations tested. This result indicates that designing for such a large lift coefficient may be a questionable procedure although it was previously indicated that the 0.4-lift-coefficient design would have a smaller trim drag at moderate lift.

It should be pointed out that only a part of the drag reduction indicated at lifting conditions for the various configurations resulted from an improvement in "drag due to lift" characteristics. This is especially true in the case of the 0.1-lift-coefficient design where most of the drag reduction at lifting conditions can be accounted for by the previously indicated reduction in drag at zero lift.

CONCLUDING REMARKS

An investigation has been made in the Langley transonic blowdown tunnel at Mach numbers between 0.8 and 1.3 to determine the possible drag reductions afforded at lifting conditions by contouring the fuselages of a sweptback-wing-fuselage combination so that the wing-fuselage surface juncture conformed approximately to the surface streamline that would exist over a wing of infinite span at a given lift coefficient. Fuselages designed for lift coefficients of 0, 0.1, and 0.4 were investigated. The results obtained from these configurations were compared with the results from an axisymmetric fuselage configuration. The longitudinal distribution of cross-sectional area of the four configurations conformed to the transonic area rule.

The results of the investigation indicated that significant drag reductions can be obtained as a result of contouring the fuselage in such a way as to satisfy the streamline shape in the wing-fuselage juncture. Drag reductions due to the streamline contouring were generally greater at lift than they were at zero lift. Of the configurations tested, the design for a lift coefficient of 0.1 generally had the lowest drag in the lift-coefficient range between 0 and 0.4 and gave reductions in drag coefficient up to about 0.007 as compared with the configuration having the axisymmetric fuselage. Except for a narrow range of Mach number and lift coefficient near design, the design for a lift coefficient of 0.4 generally had the highest drag of the three streamline configurations investigated.

The lift and pitching-moment characteristics of the four configurations tested were essentially the same with the exception of the design for a lift coefficient of 0.4 which exhibited a greater lift-curve slope C_{L_α} in the Mach number range between about 0.9 and 1.25 and more negative values of pitching-moment slope dC_m/dC_L at the supersonic Mach numbers. The design for a lift coefficient of 0.4 also exhibited a

shift in the pitching moment at zero lift which was in the direction to reduce the trim drag of the configuration.

Langley Aeronautical Laboratory,
National Advisory Committee for Aeronautics,
Langley Field, Va., March 30, 1956.

REFERENCES

1. Howell, Robert R., and Braslow, Albert L.: An Experimental Study of a Method of Designing the Sweptback-Wing—Fuselage Junctionure for Reducing the Drag at Transonic Speeds. NACA RM L54L31a, 1955.
2. Howell, Robert R.: Experimental Study of a Method of Designing the Sweptback-Wing—Fuselage Junctionure to Reduce the Drag at Moderate Supersonic Speeds. NACA RM L55H05a, 1956.
3. Whitcomb, Richard T.: A Study of Zero-Lift Drag-Rise Characteristics of Wing-Body Combinations Near the Speed of Sound. NACA RM L52H08, 1952.
4. Wright, Ray H., and Ward, Vernon G.: NACA Transonic Wind-Tunnel Test Sections. NACA RM L8H06, 1948.

TABLE I.- ORDINATES OF BODY DESIGNED FOR $C_L = 0.1$

[Body cross-section is in the shape of an ellipse]

x, in.	radius, in.	Upper half		Lower half	
		h, in.	w, in.	h, in.	w, in.
0.000	0.000				
.010	.037				
.040	.075				
.090	.112				
.160	.150				
.250	.187				
1.000	.375				
1.500	.459				
2.000	.530				
2.500	.592				
3.000	.649				
3.500	.700				
4.000	.740				
4.500	.750				
4.810		0.750	0.750	0.750	0.750
5.135		.772	.726	.737	.759
5.385		.774	.702	.724	.751
5.760		.773	.665	.705	.731
6.385		.780	.624	.697	.698
6.885		.744	.625	.667	.698
7.260		.699	.630	.632	.697
7.510		.673	.626	.615	.684
7.885		.634	.614	.596	.653
8.260		.606	.598	.584	.621
8.635		.579	.479	.567	.591
9.010		.565	.565	.565	.565
9.435		.542	.542	.542	.542
10.000		.510	.510	.510	.510

TABLE II.- ORDINATES OF BODY DESIGNED FOR $C_L = 0.4$

[Body cross-section is in the shape of an ellipse]

x, in.	radius, in.	Upper half		Lower half	
		h, in.	w, in.	h, in.	w, in.
0.000	0.000				
.010	.037				
.040	.075				
.090	.112				
.160	.150				
.250	.187				
1.000	.375				
1.500	.459				
2.000	.530				
2.500	.592				
3.000	.649				
3.500	.700				
4.000	.740				
4.500	.750				
4.810		0.7480	0.7362	0.7480	0.7672
5.135		.7280	.6918	.7280	.8485
5.385		.7230	.6266	.7230	.8817
5.760		.7000	.5784	.7000	.8946
6.385		.6830	.5392	.6830	.8853
6.885		.6530	.5418	.6530	.8826
7.260		.6140	.5522	.6140	.8825
7.510		.5940	.5601	.5940	.8575
7.885		.5780	.5708	.5780	.7772
8.260		.5840	.5788	.5840	.6623
8.635		.5700	.5790	.5700	.5978
9.010		.5640	.5650	.5640	.5650
9.435		.5420	.5420	.5420	.5420
10.000		.5110	.5100	.5110	.5100

Wing characteristics

Aspect ratio = 4.0

Taper ratio = 0.6

Section parallel to stream NACA 65A006

Area (sq.inches) = 12.96

\bar{c} (inches) = 1.838

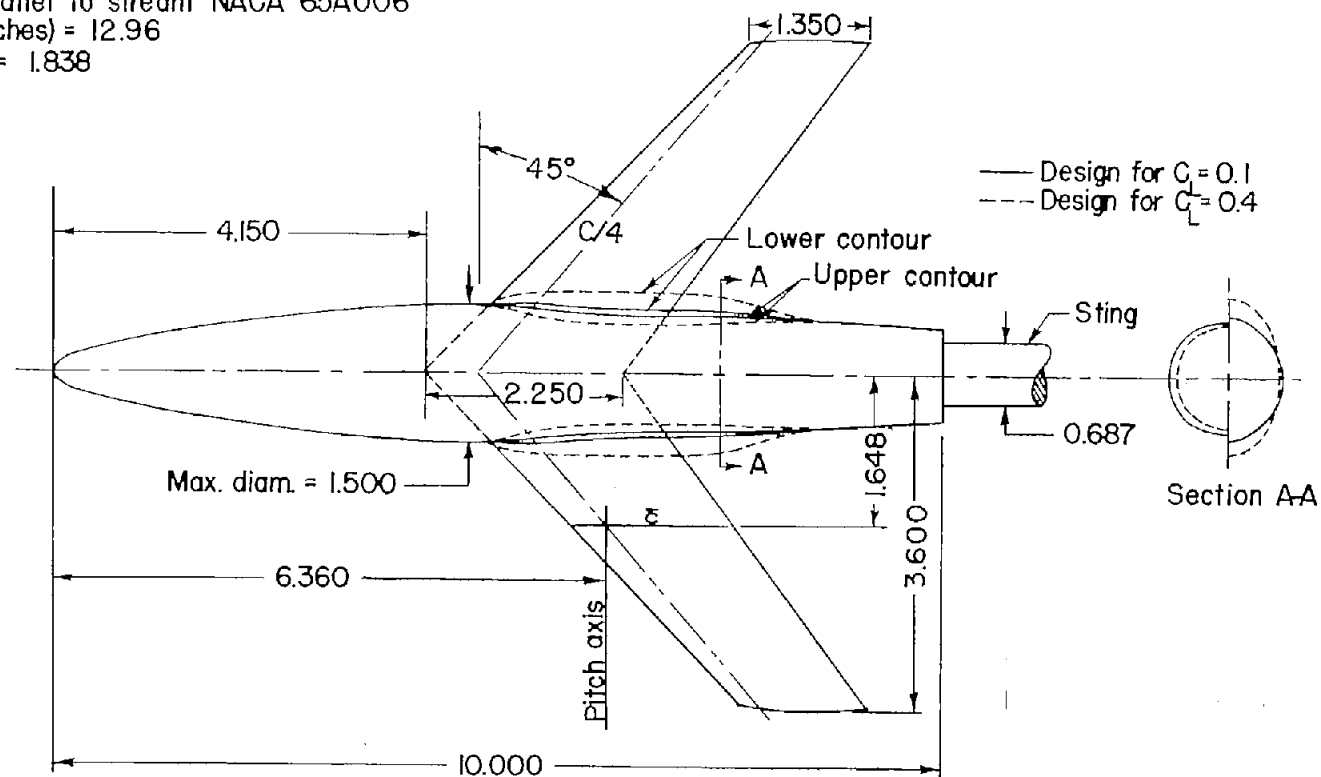


Figure 1.- Plan form of the models designed for lift. All dimensions are in inches.

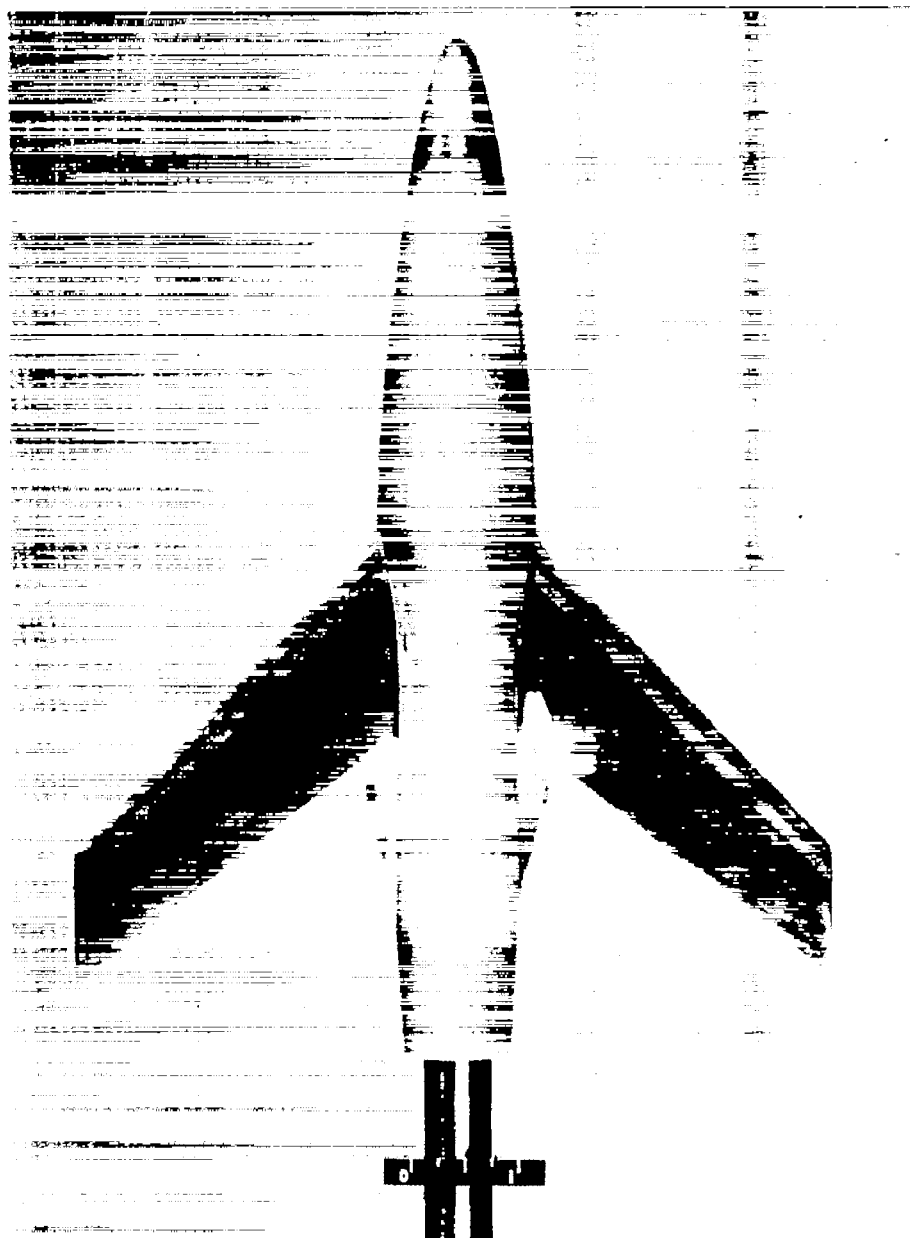


(a) $C_{L_{\text{design}}} = 0.1$.

L-88535

Figure 2.- Plan view photographs of models with contour designed for lift coefficients of 0.1 and 0.4.

CONFIDENTIAL



(b) $C_{L_{\text{design}}} = 0.4.$

L-89945

Figure 2.- Concluded.

CONFIDENTIAL

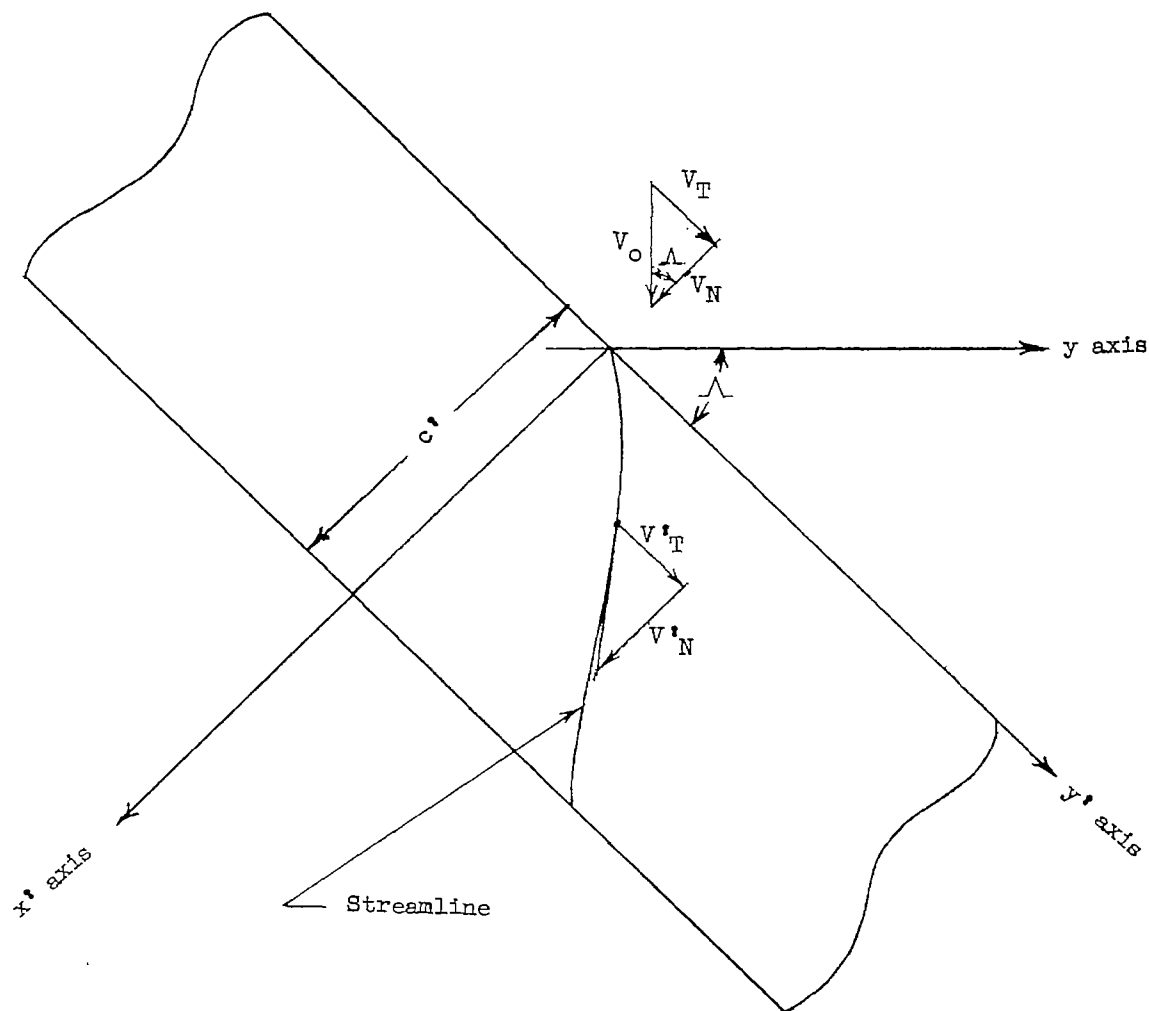
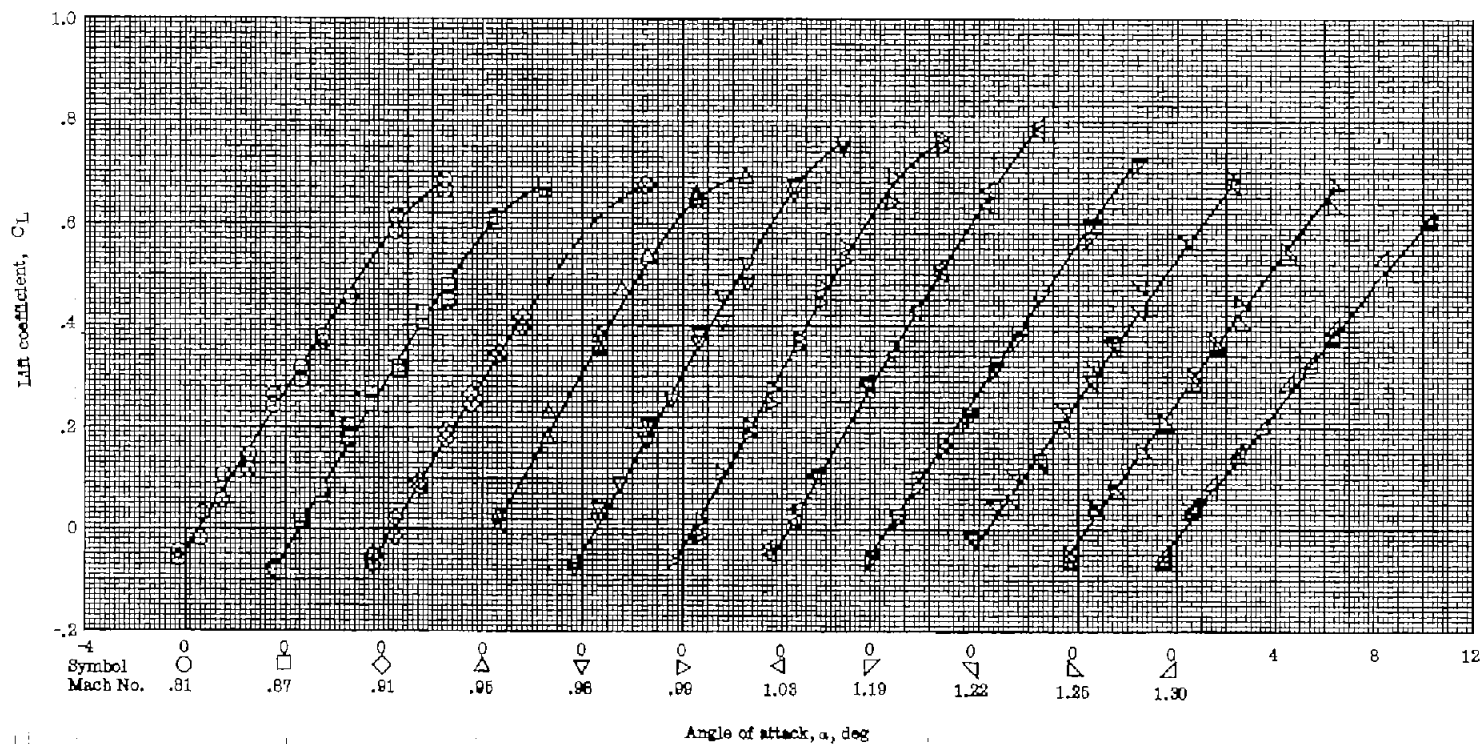
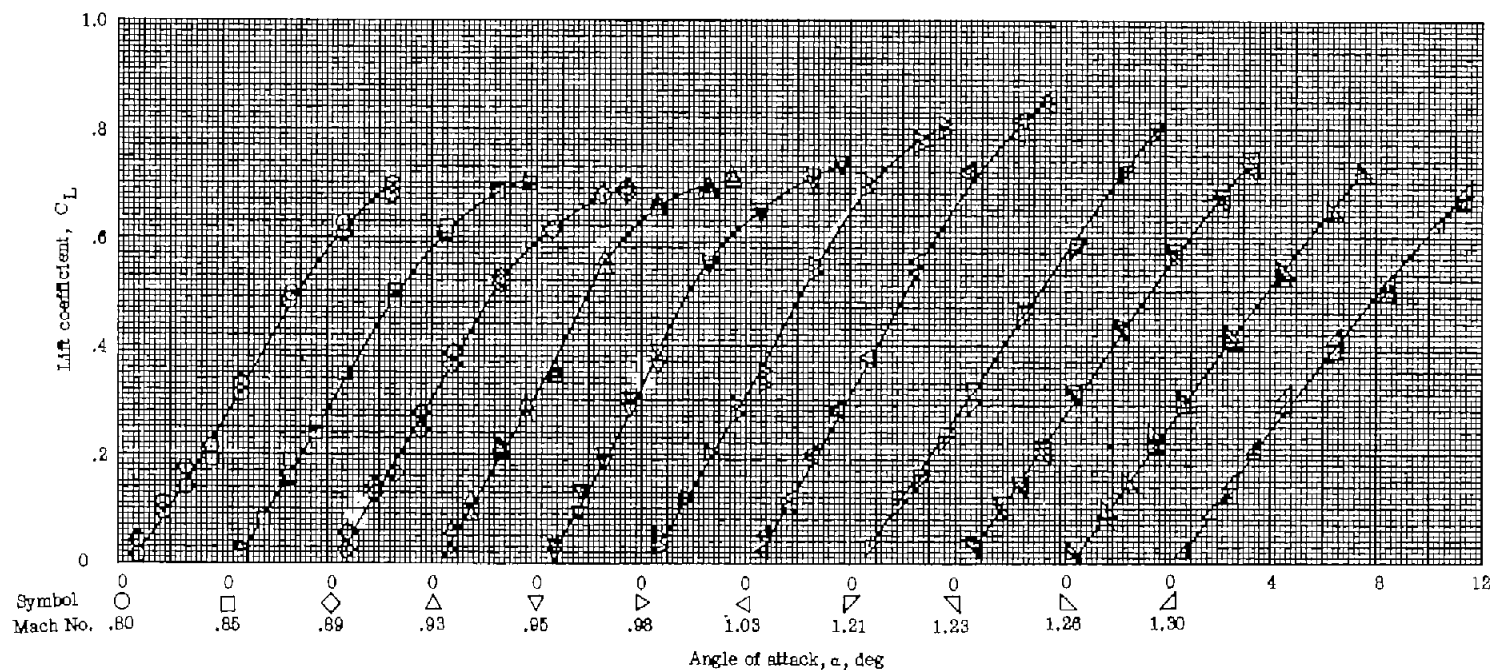


Figure 3.- Sketch showing axis system and velocity components used in the calculation of the streamline over an infinite yawed wing.



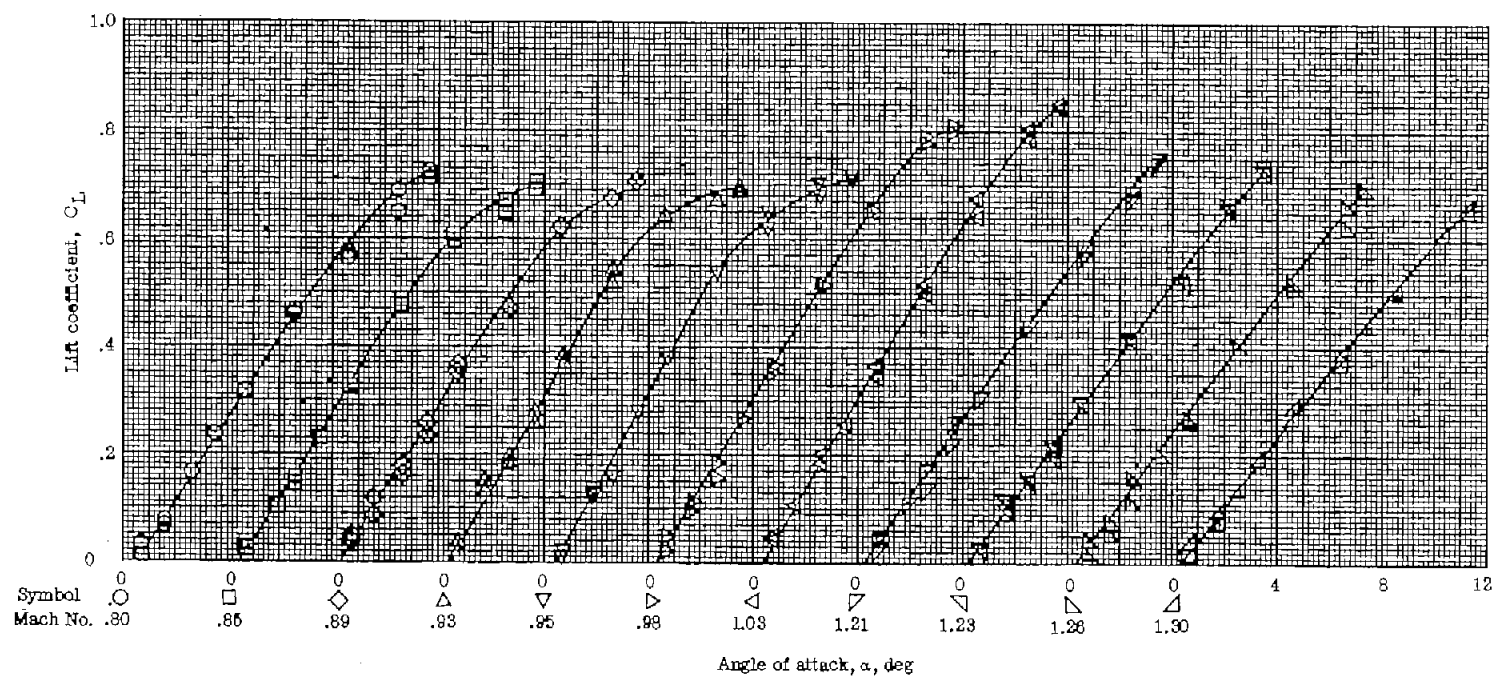
(a) Wing body incorporating only the area rule.

Figure 4.- Variation of lift coefficient with angle of attack at various Mach numbers.



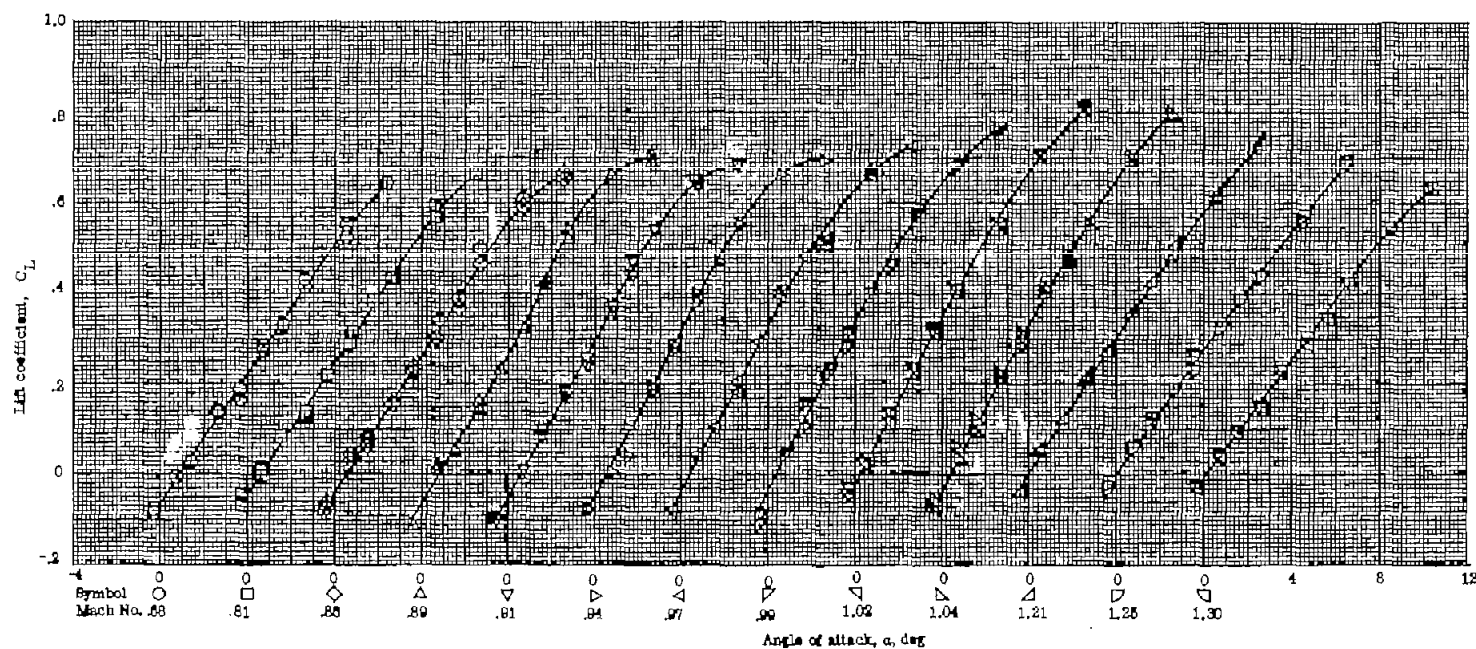
(b) Wing body designed for $C_L = 0$.

Figure 4.- Continued.



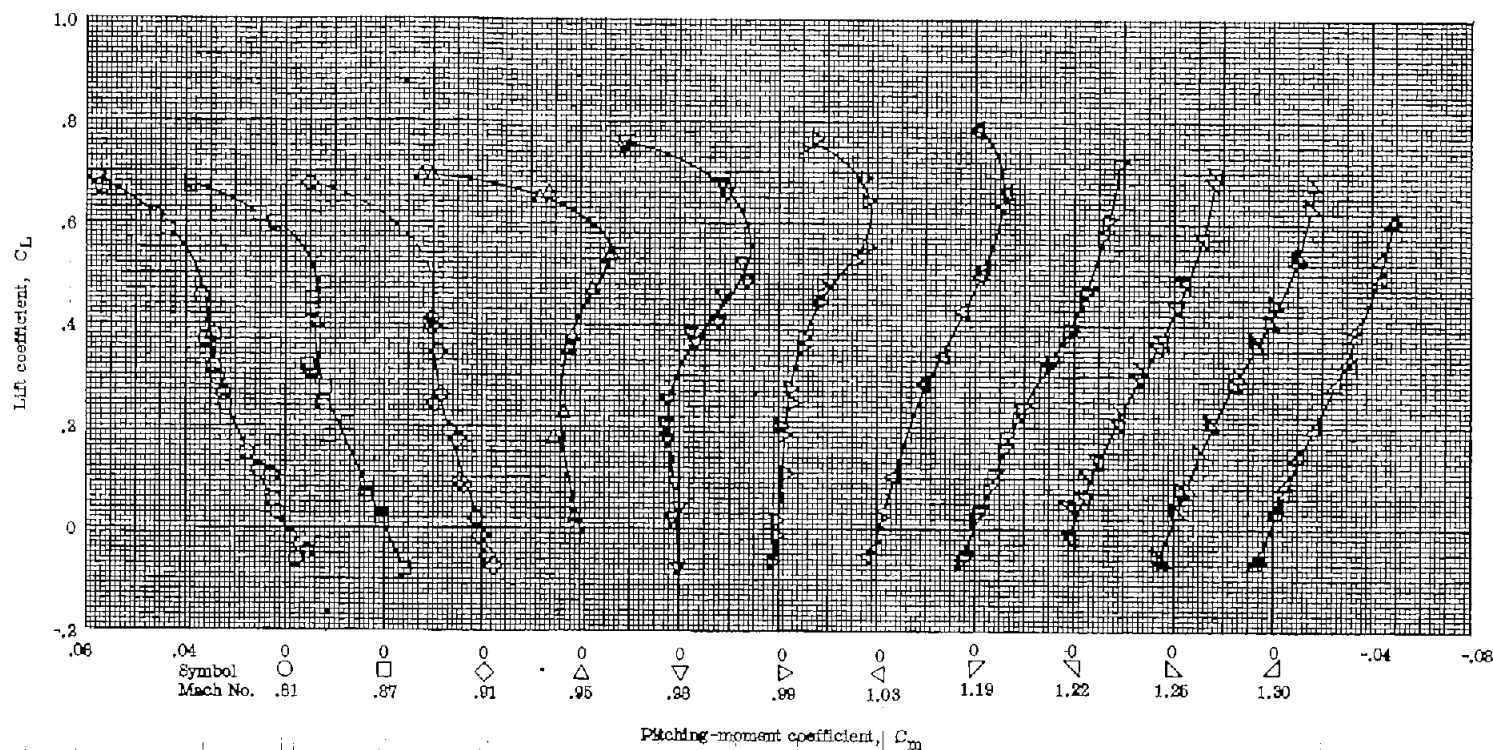
(c) Wing body designed for $C_L = 0.1$.

Figure 4.- Continued.



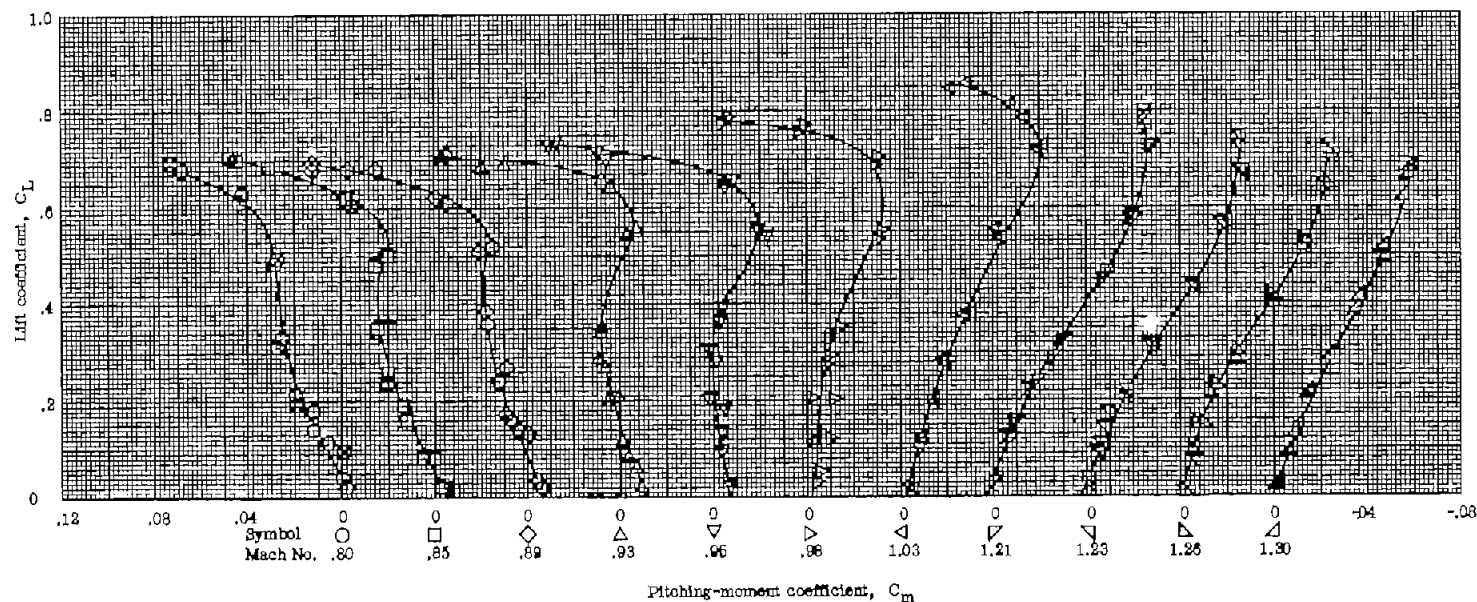
(d) Wing body designed for $C_L = 0.4$.

Figure 4.- Concluded.



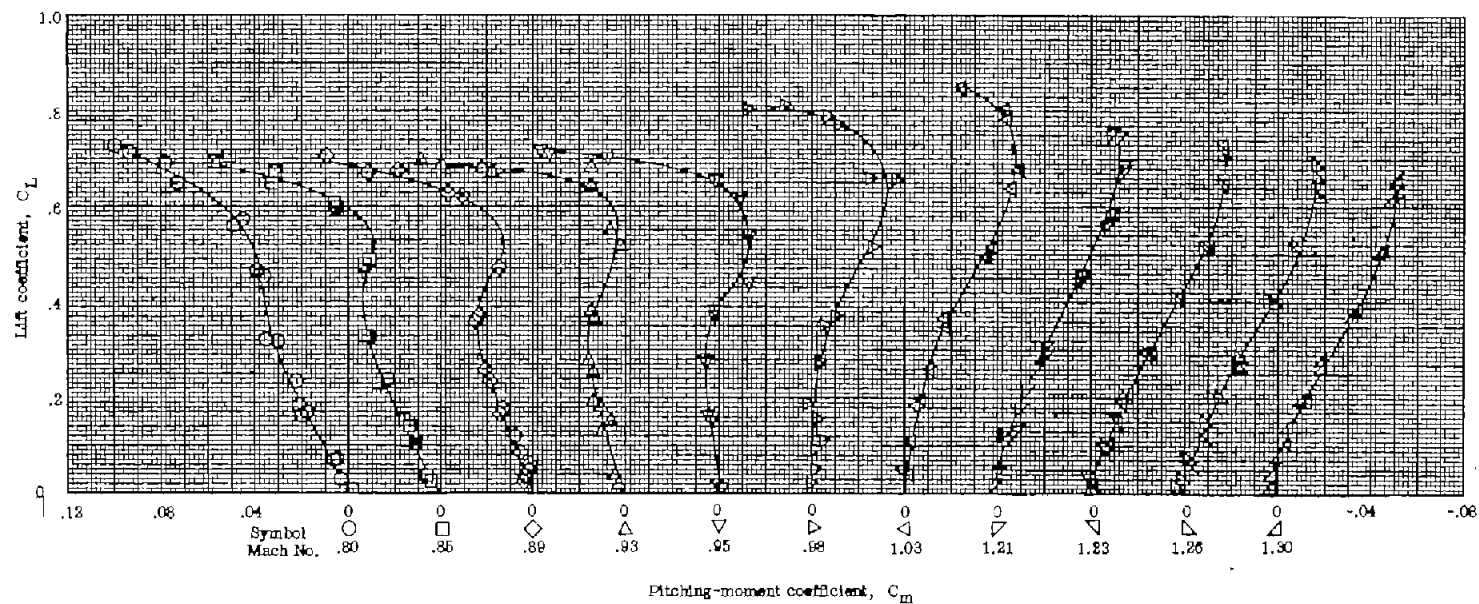
(a) Wing-body incorporating only the area rule.

Figure 5.- Variation of pitching-moment coefficient with lift coefficient at various Mach numbers.



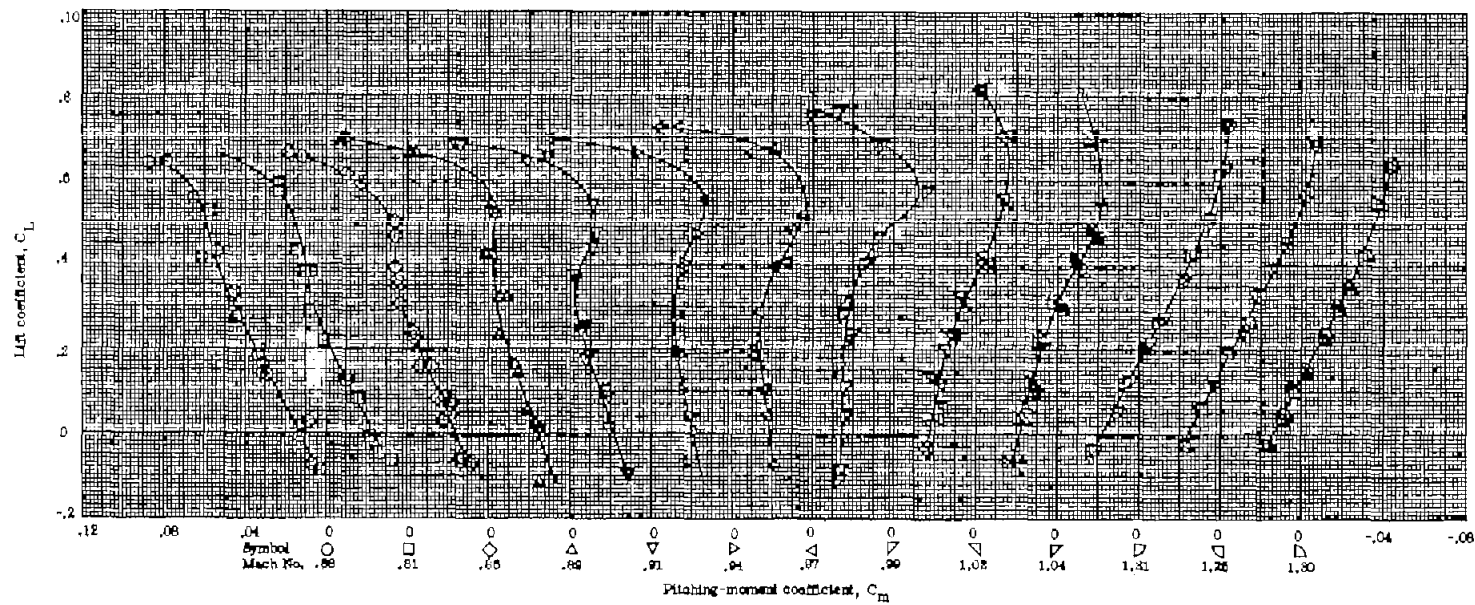
(b) Wing body designed for $C_L = 0$.

Figure 5.- Continued.



(c) Wing body designed for $C_L = 0.1$.

Figure 5.- Continued.



(d) Wing body designed for $C_L = 0.4$.

Figure 5.- Concluded.

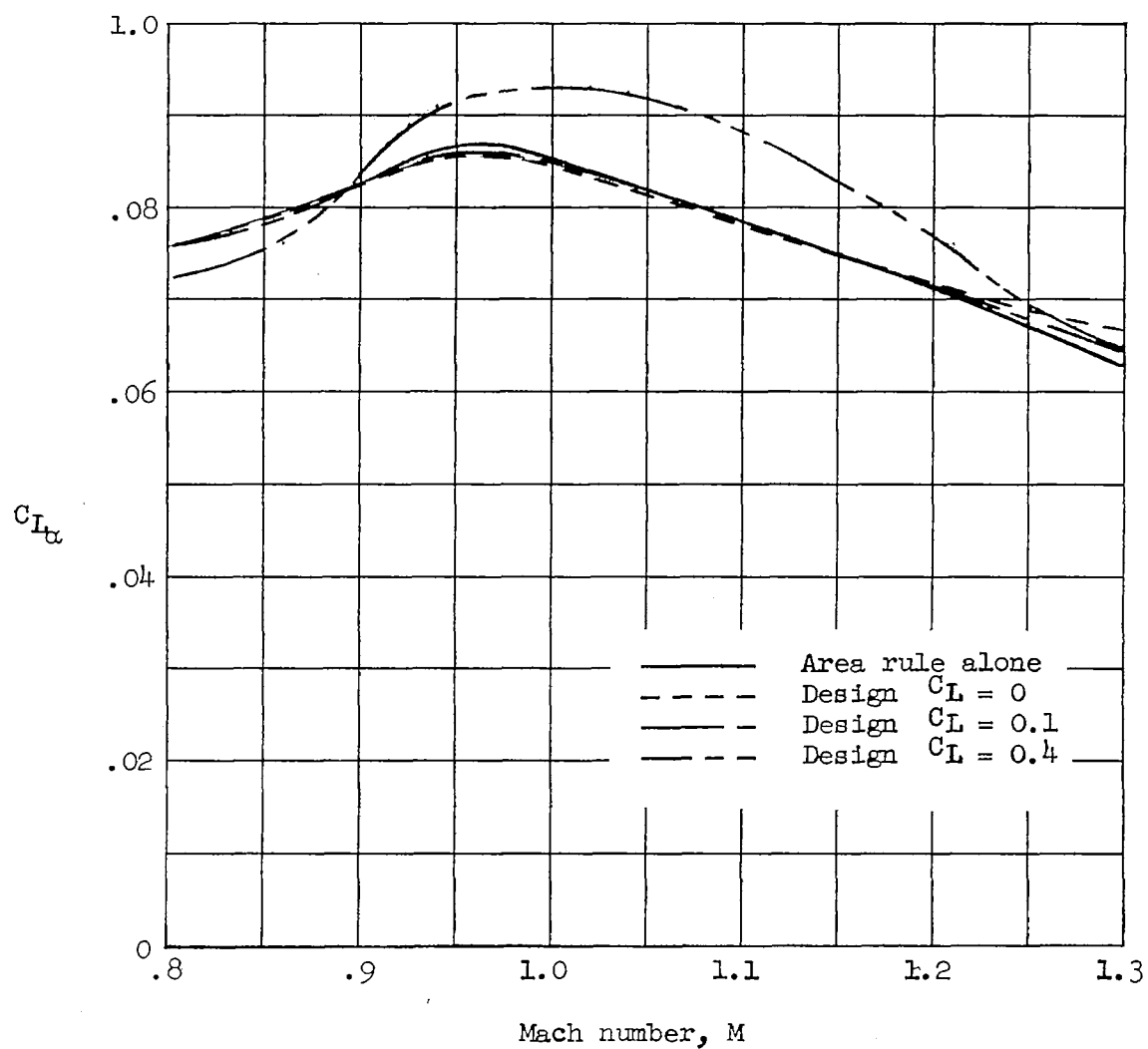


Figure 6.- Variation of lift-curve slope with Mach number for the four configurations.

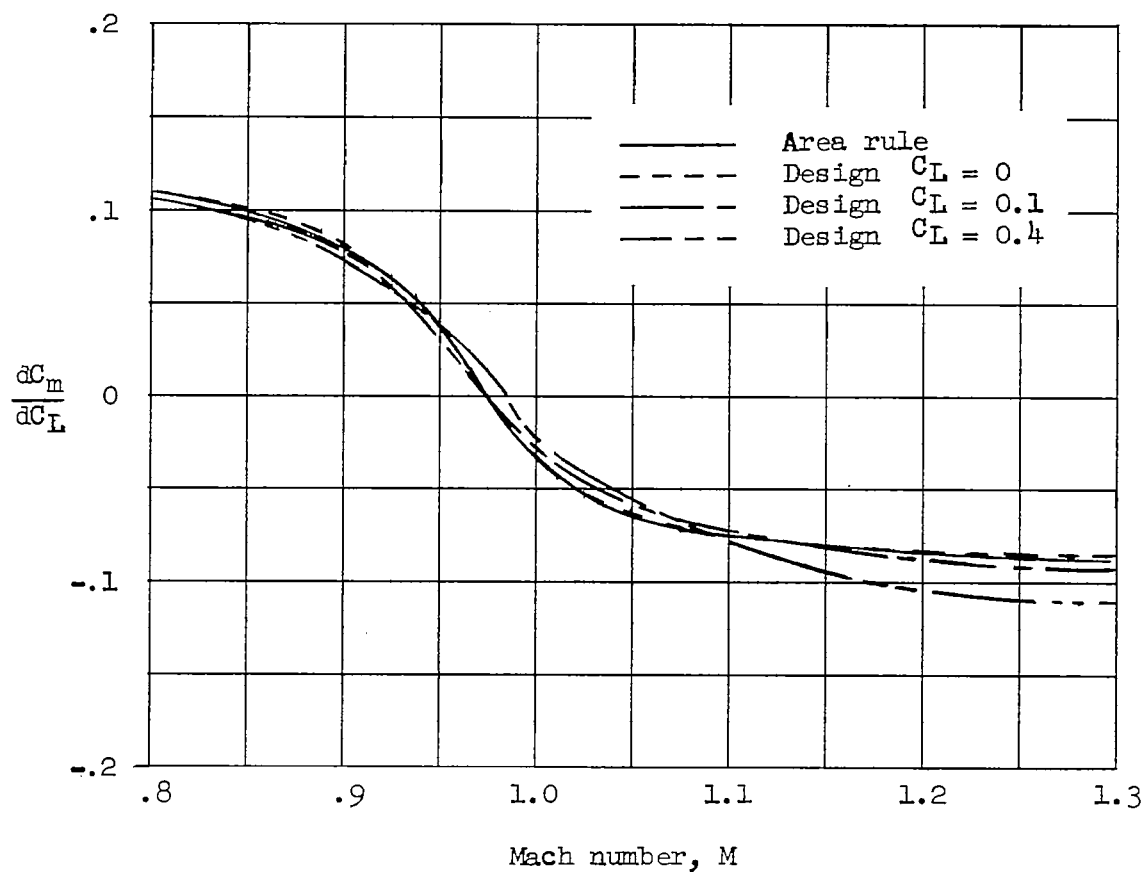
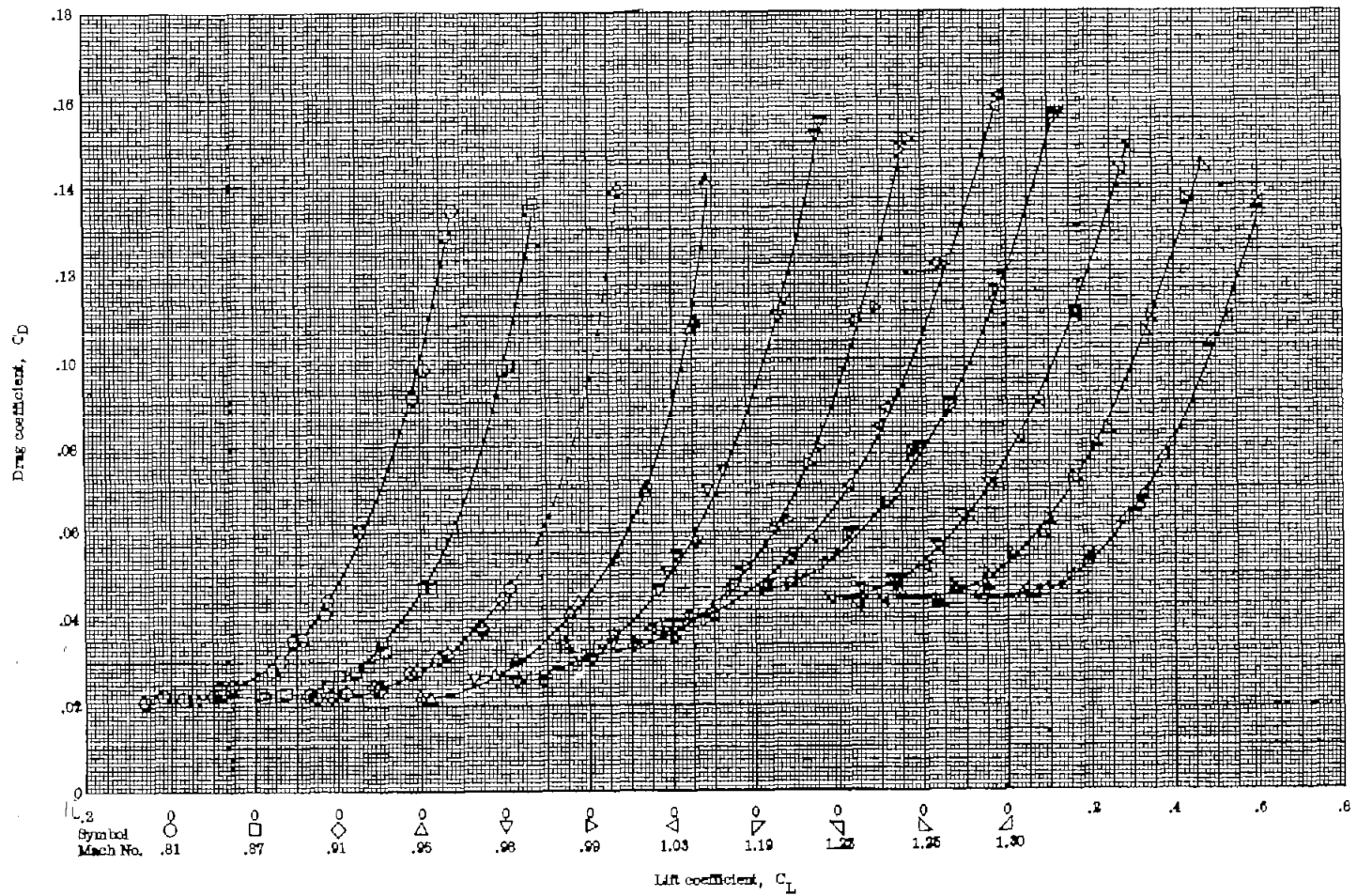
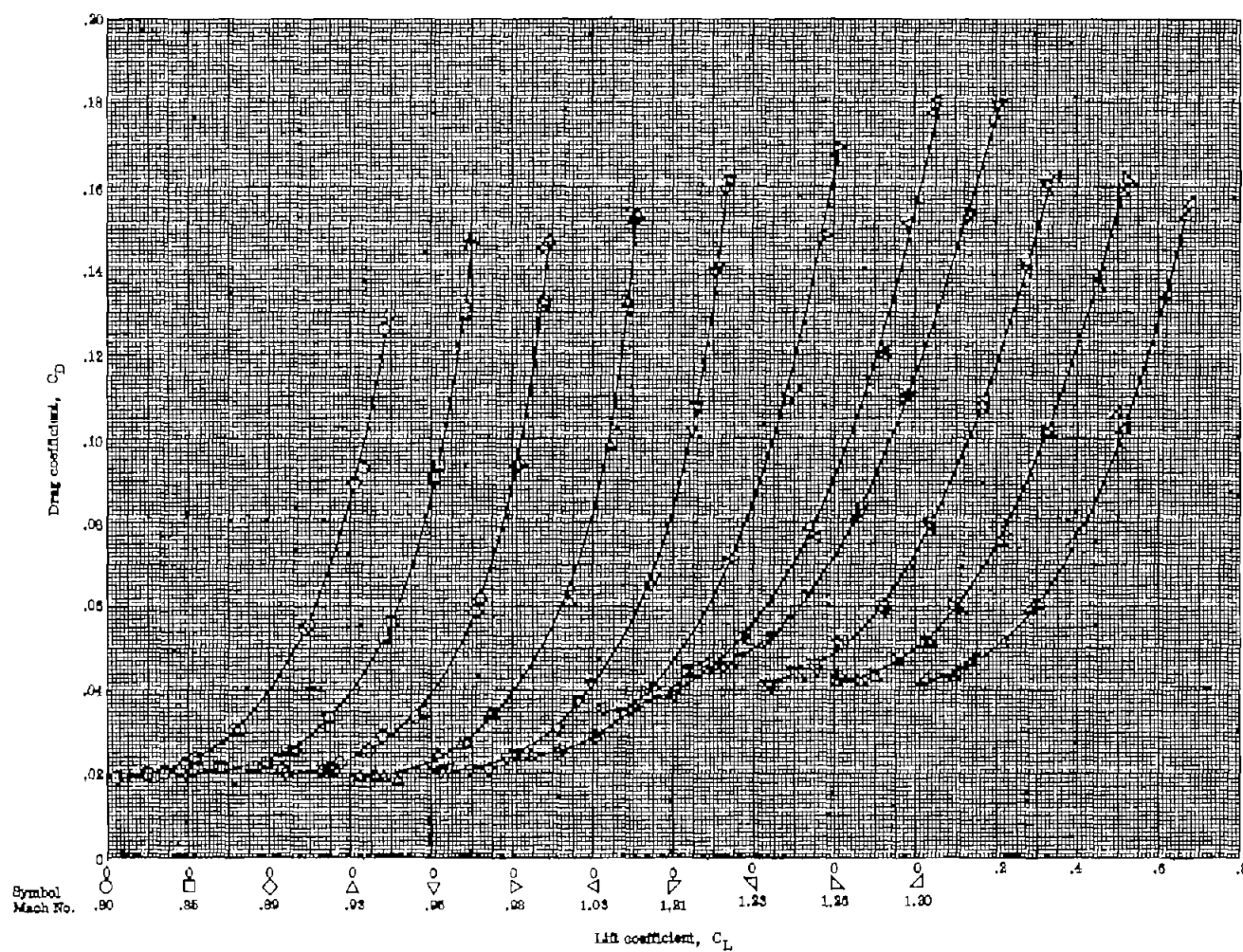


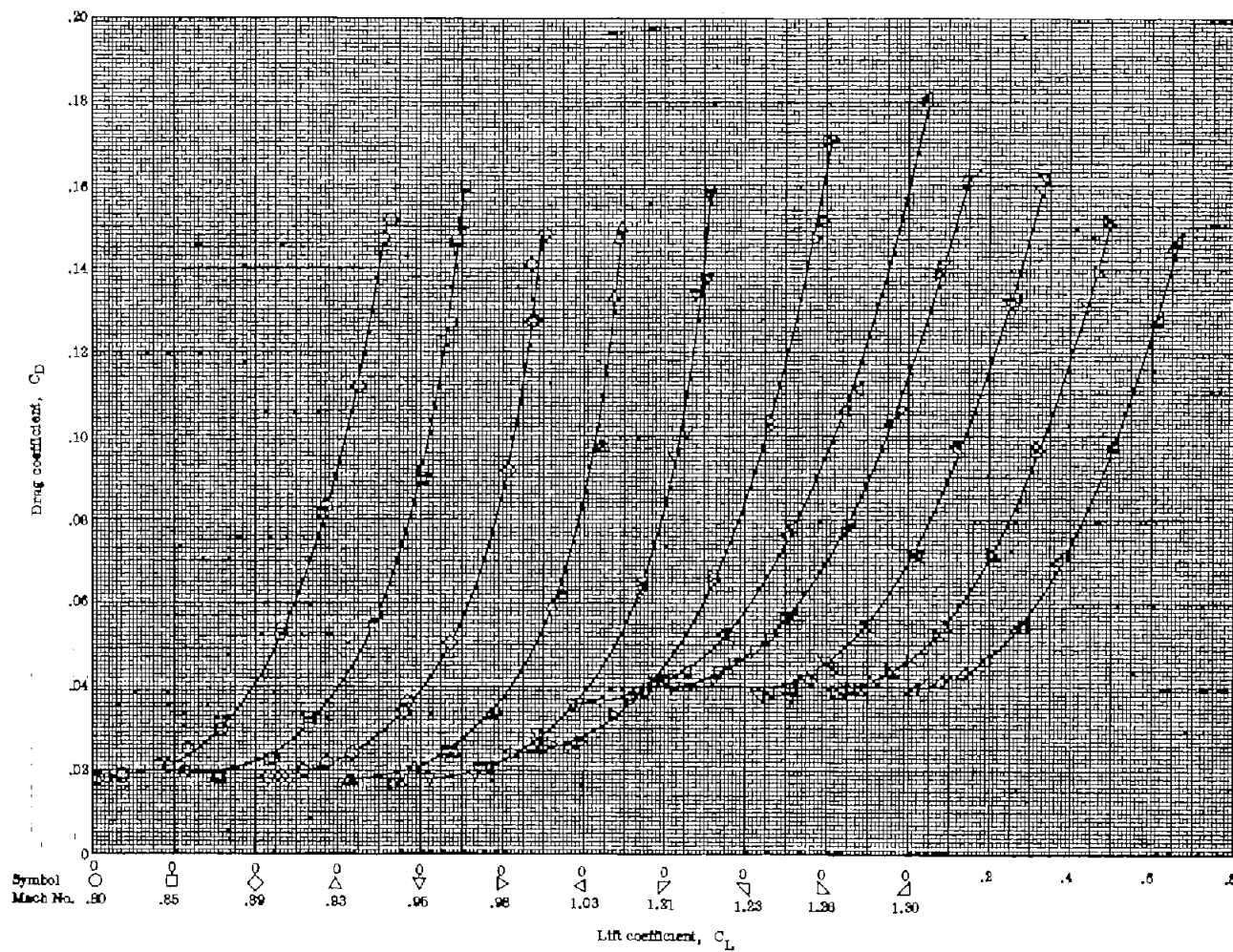
Figure 7.- Variation of pitching-moment slope with Mach number for the four configurations.



(a) Wing body incorporating only the area rule.

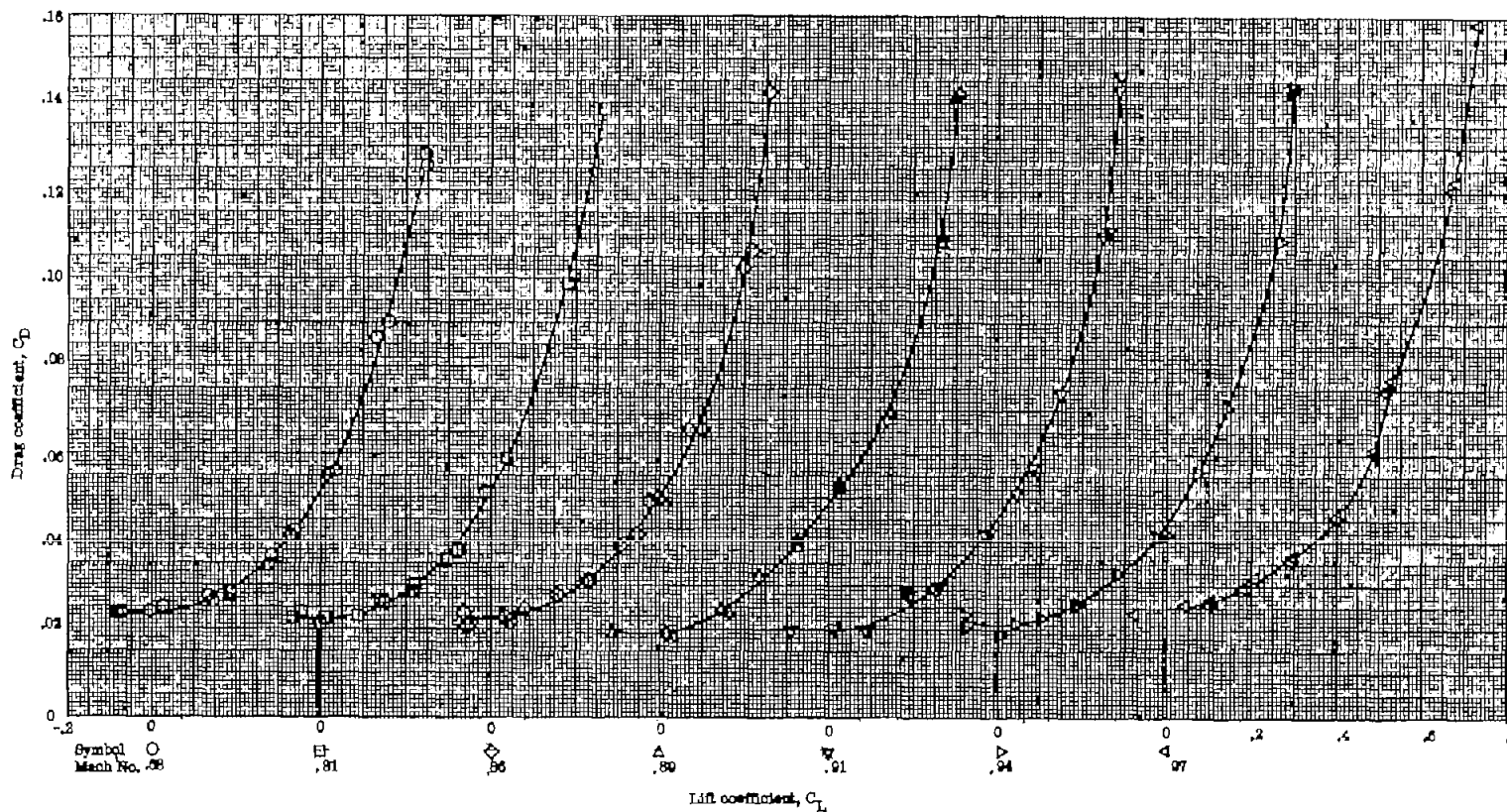
Figure 8.- Variation of drag coefficient with lift coefficient at various Mach numbers.





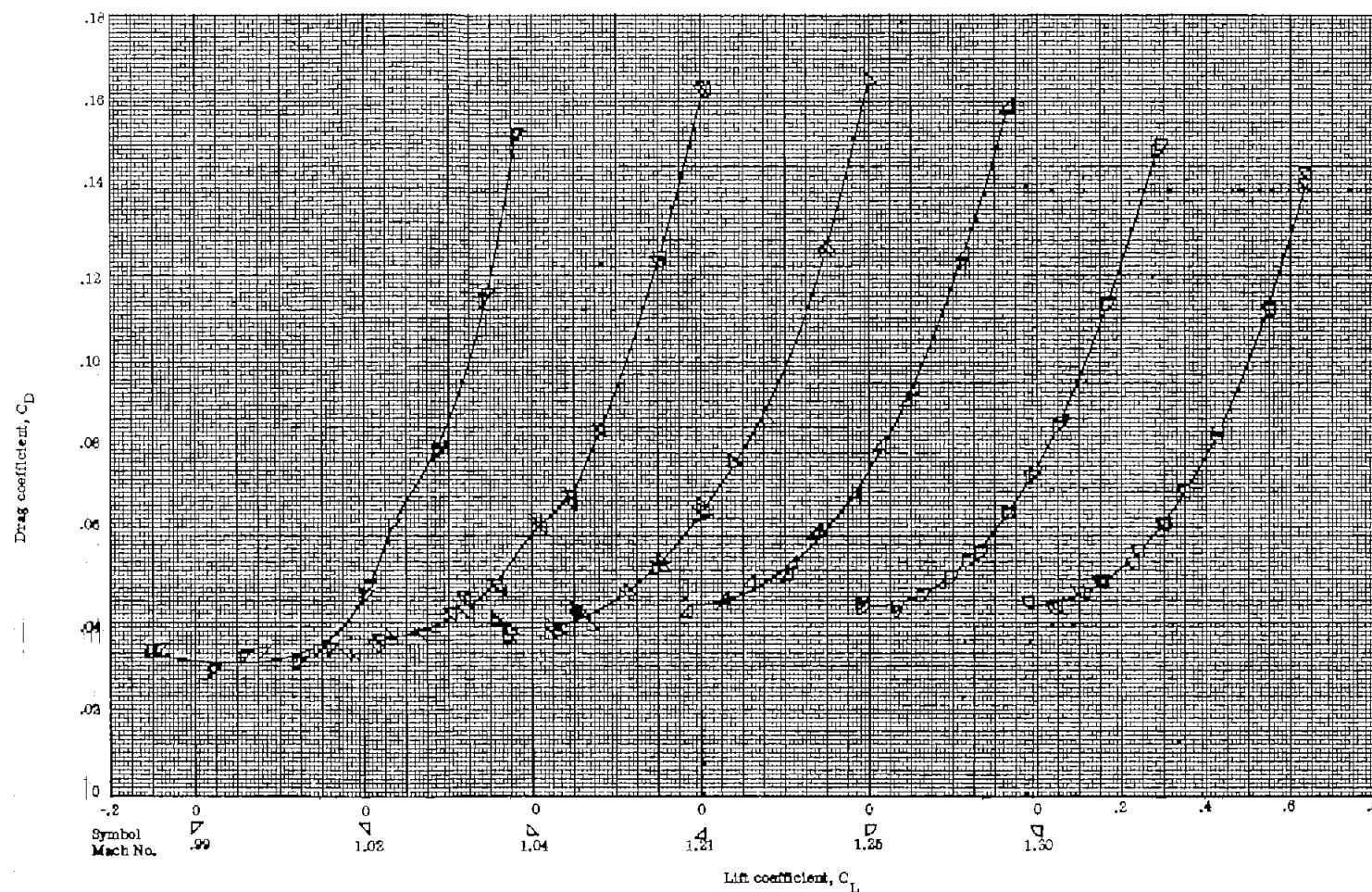
(c) Wing body designed for $C_L = 0.1$.

Figure 8.- Continued.



(d) Wing body designed for $C_L = 0.4$; Mach numbers 0.68 to 0.98.

Figure 8.- Continued.



(e) Wing body designed for $C_L = 0.4$; Mach numbers 0.99 to 1.30.

Figure 8.- Concluded.

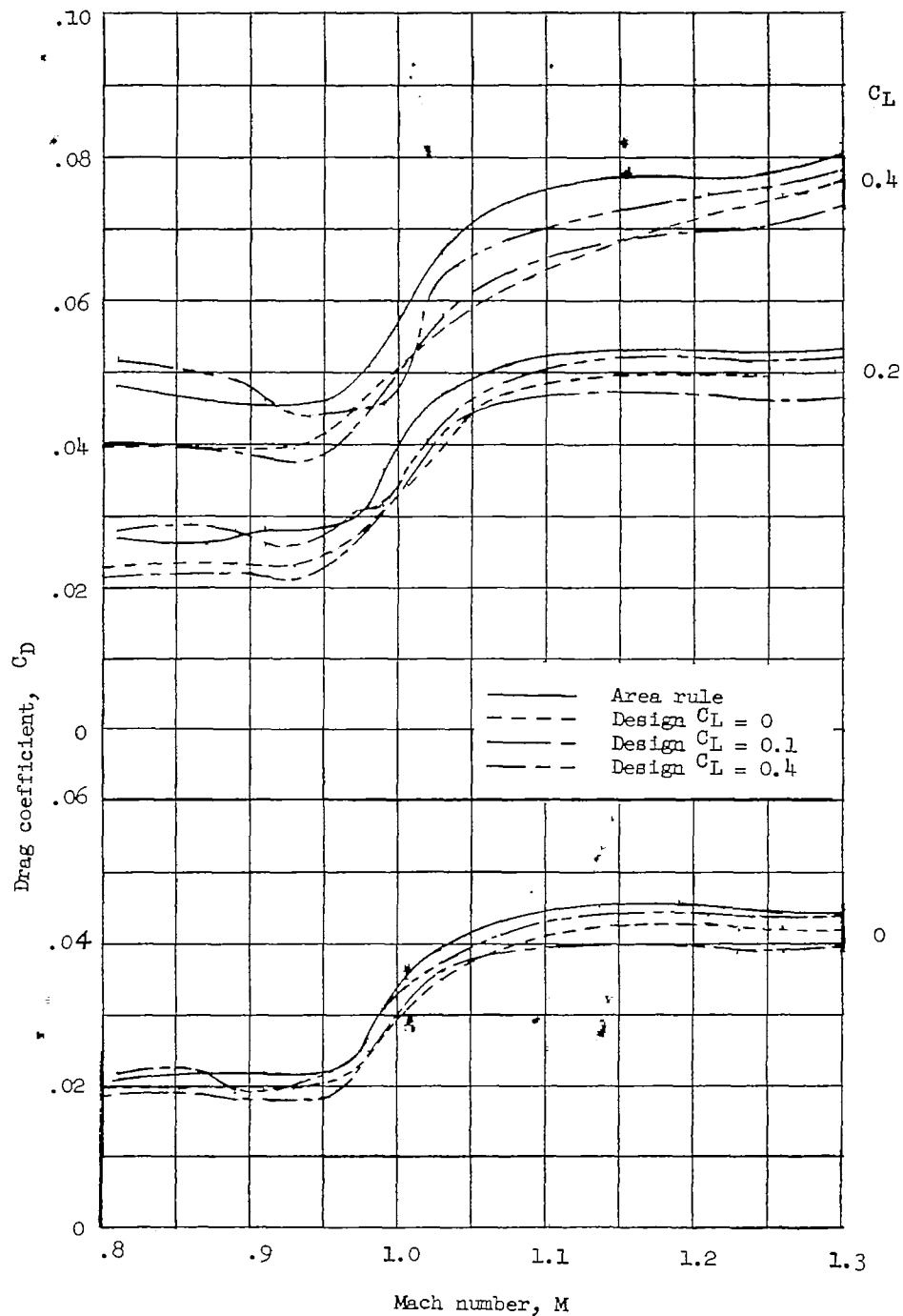


Figure 9.- Variation of drag coefficient with Mach number at lift coefficients of 0, 0.2, and 0.4.

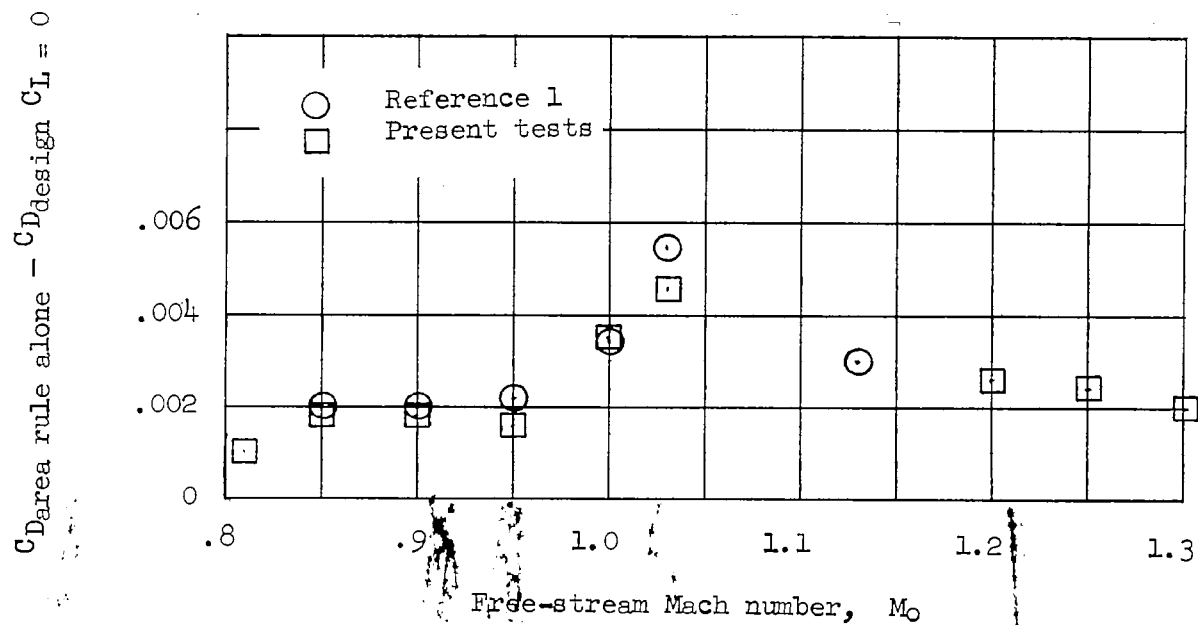


Figure 10.- Comparison of the variation with Mach number of the difference in drag between the area-rule configuration and the configuration designed for $C_L = 0$.